(In press in JGR; Accepted February 2003)

In-situ measurements of HCN and CH_3CN over the Pacific Ocean: Sources, sinks, and budgets

H. B. Singh[1], L. Salas[1], D. Herlth[1], R. Kolyer[1], E. Czech[1], W. Viezee[1], Q. Li[2], D. J. Jacob[2], D. Blake[3], G. Sachse[4], C. N. Harward[4], H. Fuelberg[5], C. M. Kiley[5], Y. Zhao[6], and Y. Kondo[7]

[1] NASA Ames Research Center, Moffett Field, CA 94035
[2] Harvard University, Cambridge, MA 02139
[3] University of California, Irvine, CA 92717
[4] NASA Langley Research Center, Hampton, VA 23665
[5] Florida State University, Tallahassee, FL 32306
[6] University of California, Davis, CA 95616
[7] University of Tokyo, Tokyo, Japan

(TRACE-P special issue, JGR-Atmospheres)
(First submitted September 2002, Accepted February 2003)

Abstract.

We report the first in-situ measurements of hydrogen cyanide (HCN) and methyl cyanide (CH_3CN, acetonitrile) from the Pacific troposphere (0-12 km) obtained during the NASA/TRACE-P airborne mission (February-April, 2001). Mean HCN and CH_3CN mixing ratios of 243±118 (median-218) ppt and 149±56 (median-138) ppt respectively, were measured. These in-situ observations correspond to a mean tropospheric HCN column of 4.2 x 10^{15} molec. cm^{-2} and a CH_3CN column of 2.5 x 10^{15} molec. cm^{-2}. This is in good agreement with the 0-12 km HCN column of 4.4 (±0.6) x 10^{15} molec. cm^{-2} derived from infrared solar spectroscopic

observations over Japan. Mixing ratios of HCN and CH_3CN were greatly enhanced in pollution outflow from Asia and were well correlated with each other as well as with known tracers of biomass combustion (e. g. CH_3Cl, CO). Volumetric Enhancement (or Emission) Ratios (ERs) relative to CO in free tropospheric plumes, likely originating from fires, were 0.34% for HCN and 0.17% for CH_3CN. ERs with respect to CH_3Cl and CO in selected biomass burning (BB) plumes in the free troposphere and in boundary layer pollution episodes are used to estimate a global BB source of 0.8±0.4 Tg (N) y^{-1} for HCN and 0.4±0.1 Tg (N) y^{-1} for CH_3CN. In comparison, emissions from industry and fossil fuel combustion are quite small (<0.05 Tg (N) y^{-1}). The vertical structure of HCN and CH_3CN indicated reduced mixing ratios in the marine boundary layer (MBL). Using a simple box model, the observed gradients across the top of the MBL are used to derive an oceanic loss rate of 8.8 x 10^{-15} g (N) cm^{-2} s^{-1} for HCN and 3.4 x 10^{-15} g (N) cm^{-2} s^{-1} for CH_3CN. An air-sea exchange model is used to conclude that this flux can be maintained if the oceans are under-saturated in HCN and CH_3CN by 27% and 6%, respectively. These observations also correspond to an open-ocean mean deposition velocity (v_d) of 0.12 cm s^{-1} for HCN and 0.06 cm s^{-1} for CH_3CN. It is inferred that oceanic loss is a dominant sink for these cyanides, and they deposit some 1.4 Tg (N) of nitrogen annually to the oceans. Assuming loss to the oceans and reaction with OH radicals as the major removal processes, a mean atmospheric residence time of 5.0 months for HCN and 6.6 months for CH_3CN is calculated. A global budget analysis shows that the sources and sinks of HCN and CH_3CN are roughly in balance but large uncertainties remain in part due to a lack of observational data from the atmosphere and the oceans. Pathways leading to the oceanic (and soil) degradation of these cyanides are poorly known but are expected to be biological in nature.

1. Introduction

Hydrogen cyanide (HCN) and methyl cyanide (CH_3CN, acetonitrile) are two of the most abundant cyanides present in the global atmosphere. Following the first spectroscopic detection of HCN in the stratosphere [Coffey et al., 1981], a number of ground and space based observations of its total atmospheric column have been made [Mahieu et al., 1995; Rinsland et al., 1998, 1999, 2000; Notholt et al., 2000; Zhao et al., 2000, 2002]. The presence of methyl cyanide was first inferred from the composition of its positive ions in the stratosphere [Arnold et al., 1978]. Limited in-situ measurements of HCN and CH_3CN have been reported from the lower stratosphere [Schneider et al., 1997]. In the stratosphere, vertical profiles of CH_3CN have also been retrieved from satellite data [Livesey et al., 2001]. Sporadic and often conflicting in-situ measurements of CH_3CN from the surface air in urban/rural environments have been published [Becker and A. Ionescu, 1982; Snider and Dawson, 1984; Hamm and Warneck, 1990]. More recently a proton transfer mass spectrometric technique has been used to measure CH_3CN in tropical environments [Crutzen et al., 2000; Reiner et al., 2001; Williams et al., 2001]. There is promise of future space-based tropospheric observations of HCN (and possibly CH_3CN) with some vertical resolution [Singh and Jacob, 2000].

Controlled studies of laboratory fires have been used to suggest that biomass burning (BB) results in significant emissions of HCN and CH_3CN into the atmosphere [Lobert, 1991, Holzinger et al., 1999]. Estimates of their global sources are highly uncertain in part due to extremely limited and often conflicting field observational data [Andreae and Merlet, 2001]. Although large quantities of HCN {≈0.40 Tg (N) y^{-1}} and smaller amounts of CH_3CN {≈0.01 Tg (N) y^{-1}} are also manufactured for applications as fumigants and chemical intermediates, their release is stringently controlled due to their known toxicity. Extremely high HCN concentrations (1-2 parts per thousand) have been reported in cigarette smoke [Verschueren, 1996]. These cyanides are expected to be slowly removed from the atmosphere by reaction with OH radicals [Cicerone and Zellner, 1983; Hamm and Warneck, 1990]. It has also been speculated that oceans may provide an important sink for CH_3CN [Hamm and warneck, 1990; Lobert, 1990; Bange and Williams, 2000], although no direct evidence of this sink is presently available. A recent modeling study by Li et al. [2000] concludes that the seasonal behavior of the total column of HCN can be reconciled with an exclusive BB source and a relatively short lifetime attributable to an oceanic sink. Measurements of cyanides in the troposphere are extremely sparse and our present knowledge of their sources, sinks, and role in atmospheric chemistry and biogeochemistry is highly uncertain.

The NASA/TRACE-P (TRAnsport and Chemical Evolution over the Pacific) airborne experiment was performed in the spring (Feb-April) of 2001 to study the composition and chemistry of the outflow of pollution from Asia to the Pacific troposphere. This experiment provided a first opportunity to utilize a recently developed technique to perform real time in-situ airborne measurements of HCN and CH_3CN. Complementing these were measurements of a large number of unique trace chemicals that are helpful in the identification of sources. Further details on the instrument payload, flight patterns, and prevailing meteorology can be found in the overview papers of Jacob et al. [this issue] and Fuelberg et al. [this issue]. Here we describe the atmospheric distribution of HCN and CH_3CN over the Pacific and use the relationship of their observed concentrations with other selected tracers to construct a first picture of their sources and sinks. We also note that these data have been further investigated by Li et al. [this issue] with the help of a global 3-D model.

2. Experimental

A Gas Chromatographic (GC) instrument, previously used to measure PAN and oxygenated organics [Singh et al, 2001 and references there in], was expanded to measure HCN and CH_3CN. This instrument was integrated aboard the DC-8 aircraft and all measurements discussed in this paper were performed on this platform. A volume of 5.0 l min^{-1} (0˚C, 1 atm.) of ambient air was drawn through a heated Teflon-lined sampling probe using a low pressure-drop mass flow controller (MKS Model 1559A). An aliquot of 200 ml of air (80 ml/min) was passed through a water dryer held at –35˚C, and then cryogenically trapped in a sample loop held at -140 ˚C. Extensive laboratory tests were performed to ensure that the water trap removed moisture without measurable loss of other constituents of interest. After cryogenic concentration, the sample loop was heated to 70˚C and switched in line with the GC columns. A 50-m “analytical” and a 15-m “stripper” DB wax (0.85 microns) quartz capillary column of 0.45 mm ID were used for constituent separation. The “stripper column” was used to back flush high boiling constituents from the system. Chemicals were detected with a Photo Ionization Detector (PID) placed in series with a Reduction Gas Detector (RGD). Only the RGD was capable of detecting cyanides while both PID and RGD were suitable for detecting oxygenates. All

calibrations were performed using standard addition techniques and in a manner that mimicked ambient air sampling. Primary standards for HCN and CH_3CN were referred to a series of permeation tubes held at 30˚C and 0˚C. A 1-ppm compressed mixture of CH_3CN in nitrogen was also used for this purpose. The detector response for CH_3CN and HCN was linear over a wide concentration range. A precision of ± 5% could be obtained on the ground in dry air. Precision under the highly variable atmospheric conditions during airborne operation was of the order of ±15% in the free troposphere and was somewhat poorer in the moist marine boundary layer (MBL). Overall measurement accuracy is expected to be ±25% with a limit of detection of 30 ppt.

A chromatogram showing the separation and detection of HCN and CH_3CN from ambient air is shown in Figure 1. The tailing of peaks in Figure 1 occurs in the mercuric oxide bed and is a known difficulty with the RGD detector. This was the first time that this instrument was used to measure ambient HCN and CH_3CN. There were some instances, usually in the early stages of sampling, when the sensitivity of the instrument appeared to be poor. This loss of sensitivity could be easily confirmed from the analysis of calibration standards. Although the causes of this loss of sensitivity are not fully understood, we have chosen to disregard data collected under such conditions. Further improvements in instrument sensitivity and precision should be possible in the future.

3. Results and Discussion

In the following sections we provide an analysis of the observations of HCN and CH_3CN during TRACE-P (February 25 to April 10, 2001). All measurements discussed in this paper were performed aboard the NASA DC-8 aircraft. The Pacific troposphere was sampled from 0.1-12 km over a region that extended from 10-45˚N latitude and 100-240˚ E longitude. More details on flight profiles and sampling density are provided in Jacob et al. [this issue]. When appropriate, this region has been divided into areas representing the western Pacific (Longitude 100-160˚E) and central/eastern Pacific (Longitude 160-230˚E). To relate these data with other key chemicals, which were measured at differing frequencies, merged data files were created. In much of the analysis that follows the 5-min merged data set has been used. Unless noted otherwise, only data from the troposphere are considered. A convenient filter (O_3>100 ppb and z >10 km or CO< 50 ppb) was used to remove stratospheric influences. We used methyl chloride and potassium as tracers of biomass combustion, and CO as a more generic tracer of pollution. Although CH_3Cl is known to have a diffuse oceanic and possibly biogenic source [Butler, 2000], it was possible to use it as a tracer of biomass/biofuel combustion in air masses downwind of its terrestrial sources. Tetrachloroethylene (C_2Cl_4), a synthetic organic chemical, was employed as a tracer of urban pollution. When appropriate, a pollution filter was used to mitigate the effect of pollution (CO<120 ppb; C_2Cl_4< 10 ppt). This filter resulted in mixing ratios of 96(±15) ppb/CO and 3(±1) ppt/C_2Cl_4, and is assumed to represent near-background conditions. Utilizing meteorological and tracer information we are able to draw important conclusions about the sources and sinks of HCN and CH_3CN.

3.1 Atmospheric Distribution

Figure 2 shows the vertical distribution of HCN and CH_3CN in the troposphere based on all TRACE-P data. Superimposed on the data are mean (± σ) mixing ratios based on 2-km bins. Mean concentrations of these and key tracer species are presented in Table 1. It is evident that substantial concentrations of cyanides are present throughout the atmosphere and that there is

significant variability. These mixing ratios correspond to a 0-12 km grand average of 243±118 ppt (median-218 ppt) HCN and 149±56 ppt (median-138 ppt) CH_3CN. Comparable in-situ HCN data from the troposphere are not available. However, our measured values in the upper troposphere (UT) are not inconsistent with the 164 (±25%) ppt lower stratospheric mixing ratios reported by Schneider et al., [1997] for February 1995. Unlike HCN, a more extensive tropospheric data base for CH_3CN has become available. Following the TRACE-P deployment, Pacific region measurements of CH_3CN were made at the Mauna Loa observatory (April, 2001) and over the eastern Pacific (April-May, 2002). These studies report mixing ratios in the vicinity of 100-200 ppt in good agreement with our results [Karl et al., 2003; De Gouw et al., 2003]. Background CH_3CN mixing ratios reported from the Indian Ocean and Surinam [Crutzen et al., 2000; Lelieveld et al., 2000; Reiner et al., 2001; Wisthaler et al., 2002] were generally in the range of 100-300 ppt. It is noted that strong seasonal variations in the atmospheric abundance of HCN (and likely CH_3CN) are present [Zhao et al., 2002], and any comparison of observations must take this factor into account.

The variability in the mixing ratios cyanides is substantial and largely associated with the outflow of pollution from the Asian continent. Maximum concentrations of 1610 ppt and 320 ppt were measured for HCN and CH_3CN, respectively. It is instructive to normalize these data with respect to a common tracer of pollution to minimize the observed scatter. Figure 3 shows the altitude profile when the mixing ratios of HCN and CH_3CN are normalized with respect to CO. An evident feature is that relative to CO, the mixing ratios of HCN and CH_3CN decline rapidly towards the surface of the ocean. A nearly identical vertical structure can also be seen when mixing ratios are normalized to a more specific tracer of BB such as CH_3Cl. This behavior is also seen directly in the vertical structure of HCN and CH_3CN (Table 2) when the data are further filtered for relatively clean atmospheric conditions (CO<120 ppb; C_2Cl_4<10 ppt). As we shall see in Section 3.5, these reduced lower tropospheric concentrations are a first indication of their surface sink.

On limited occasions and at mid-latitudes, it was possible to penetrate the lowermost part of the stratosphere. Ozone concentrations as large as 600 ppb were measured during these episodes. Figure 4 shows the distribution of CH_3CN plotted as a function of O_3. The decline in CH_3CN concentrations above the tropopause is very similar to that observed by Schneider et al., [1997]. It was not possible to collect sufficient HCN data in the stratosphere due to an instrument artifact.

3.2 Atmospheric Columns

For the sampled latitudes and season, our in-situ measurements (Table 1) correspond to a 0-12 km tropospheric HCN column of 3.7-4.2 x 10^{15} molec. cm^{-2} and a CH_3CN column of 2.4-2.5 x 10^{15} molec. cm^{-2}. The lower end of this range is based on median mixing ratios while the upper end is based on means. This result can be best compared with the Japanese ground-based infrared solar spectroscopic observations of the column of HCN over Tsukuba (36.2˚N), Rikubetsu (43.5˚N), and Moshiri (44.4˚N) during the TRACE-P period. Mean 0-12 km column densities (in units of 10^{15} molec. cm^{-2}) of 4.8±0.7, 4.1±0.4, 4.4±0.6 respectively, were derived. The daily HCN columns from these sites are shown in Figure 5. These mean column densities of 4.1-4.8 x 10^{15} molec. cm^{-2} are in reasonably good agreement with the derived mean HCN column of 4.2 x 10^{15} molec. cm^{-2} deduced from in-situ measurements (Figure 5). Although there can be substantial year to year variability, typical spring time column densities of 4-5 x 10^{15} molec. cm^{-2} have been reported from 1996 to 2000 over Japan [Zhao et al., 2000; 2002]. HCN columns have

also been derived from spectra collected at high altitude observatories located at Mauna Loa, Hawaii (19.5˚N, 3.4 km altitude) and Jungfraujoch, Switzerland (46.6˚N; 3.6 km altitude) [Rinsland et al. 1999, 2000]. Mean spring-time HCN columns from these locations are found to be in the range of 2-3 x 10^{15} molec. cm^{-2}. Once again, this is in reasonable agreement with the 3.5-12 km mean column density of 2.4 x 10^{15} molec. cm^{-2} derived from the present in-situ measurements (Table 1). We note that the ground-based spectroscopic observations do not have sufficient vertical resolution to determine the boundary layer HCN column. Long-term spectroscopic observations are inconclusive about any possible trend in the atmospheric HCN [Mahieu et al., 1997; Rinsland et al., 2001]. Similar spectroscopic data for CH_3CN are not available possibly because its strongest absorption in the 6-μm region is obscured by water vapor.

3.3 Tracer Relationships

Despite a high degree of variability, mixing ratios of HCN and CH_3CN are related suggesting common sources. Figure 6 shows this relationship in the free troposphere (>2.5 km) over the entire Pacific. A linear relationship provides a reasonable fit to these data (R=0.70) which is somewhat improved with a second order best fit (R=0.77). The latter suggests that under certain conditions emissions of HCN increase more rapidly than CH_3CN. While there is insufficient data to draw firm conclusions, there is an indication that these mixing ratios are non-linearly related. A likely cause is that emission factors of HCN and CH_3CN vary differently with the nature of fuel and combustion temperature. There is insufficient knowledge about the pyrogenic formation mechanisms of cyanides to quantitatively understand the nonlinear behavior. There exists a linear relation between CH_3Cl, a tracer of biomass combustion, and HCN, CH_3CN, and CO in the free troposphere over the western Pacific as well as the central/eastern Pacific regions (Figure 7). These linear relationships are maintained over the entire Pacific troposphere. Figure 8 demonstrates the persistence of this linear relationship between cyanides and tracer (CO and CH_3Cl) mixing ratios in the UT (8-12 km). The somewhat improved linear correlations over the central/eastern Pacific as well as the UT are attributable to the greater homogeneity of the air masses farther away from their sources. In their entirety, these relationships provide broad support for the view that the atmospheric burden of cyanides is strongly associated with BB sources. Nonvolatile aerosols also behaved in a manner similar to gas phase tracers such as CO.

The linear relationships typically observed in the free troposphere frequently broke down in the boundary layer in part due to the high complexity of the Asian anthropogenic sources and the proximity of the oceanic sink. We sampled two distinct outflow events when low level outflow (<1 km) of pollution was encountered in the Taiwan Straits (Mission 12) and the Yellow Sea (Mission 13). Trajectory analysis showed that the Taiwan Straits episode was impacted by source regions from the Fujian province of China while the Yellow Sea episode was a direct outflow from the Shanghai urban complex. Figure 9 shows the relationship of CH_3Cl with cyanides and CO for these missions. Extremely large concentrations of CH_3Cl were associated with virtually no elevation in CH_3CN and only a modest increase in HCN. A very large fraction (≈ 30%) of fuel consumed in China is from the use of biofuels/coal. We interpret the boundary layer outflow data to infer that such fuels are inefficient producers of cyanides. A low fuel nitrogen content and a high halogen content is implied.

3.4 Source Estimates of HCN and CH_3CN from Biomass Burning

To assess the sources of cyanides, we investigated their atmospheric behavior relative to known tracers of combustion and urban pollution. As a first step we looked at the Enhancement Ratios (ERs) of HCN and CH_3CN relative to CH_3Cl and CO in several plumes sampled in the free troposphere (>3 km) and in episodes of pollution outflow in the MBL (0-1 km). These data are summarized in Table 3. All these chemicals are long lived (several months) and the plumes are sufficiently fresh (<5 days), that chemical changes during transport should have a negligible effect on these ERs. Therefore these Enhancement Ratios are effectively the same as Emission Ratios defined by Andreae and Merlet [2001]. Five-day back trajectory analysis [Fuelberg et al., this issue], indicated that the free tropospheric plumes generally originated over regions of southern China, southeast Asia, and northern Africa. Satellite observations showed that fires were prevalent in these regions. It is common knowledge that BB air masses are easily advected into the free troposphere. All of the relevant tracers of biomass combustion (e. g. HCN, CH_3CN, CO, CH_3Cl, and K) were significantly elevated in these plumes. Additionally, the elevation in C_2Cl_4 (Table 3) was quite small (0-10 ppt). In contrast, trajectories associated with the 9 boundary layer pollution episodes (Table 3), showed that nearly all of them had crossed the eastern China coastal areas at relatively low altitudes within the last two days. These episodes were also associated with high concentrations of C_2Cl_4 and other anthropogenic tracers.

Fossil fuel combustion is not a known source of either CH_3Cl or cyanides. Because of this specificity, we will first use ERs with respect to CH_3Cl to assess BB emissions of HCN and CH_3CN. In large east Asian cities, most of the BB emissions are due to biofuels [Streets and Waldhoff, 1998; Yevich and Logan, 2003], and thus boundary layer ERs provide an indicator of cyanide emissions from this source. In the following analysis we use both free tropospheric and MBL ERs to estimate the total BB source of HCN and CH_3CN. The former represents relative emissions from plumes due to fires, and the latter indicates biofuel/coal emissions. We adopt a global BB CH_3Cl source of 0.9 Tg y^{-1} (87% biomass fires; 13% biofuels/charcoal) based on the most recent evaluations [Lobert et al., 1999; Andreae and Merlet, 2001]. To obtain global BB source of HCN and CH_3CN ($S_{HCN,CH3CN}$, Tg (N) y^{-1}) we scale ER's in Table 1 (ppt/ppt) according to Equation 1.

$$[S_{HCN,CH3CN}]_{CH3Cl} = 0.9 \times \{14/50.5\} \times \{0.87 \times ER_{ft} + 0.13 \times ER_{bl}\}_{CH3Cl} \qquad (1)$$

where ER_{ft} and ER_{bl} are the respective ERs (ppt/ppt) with respect to CH_3Cl in the free troposphere and the MBL (Table 1). To minimize errors due to urban influences, only ER_{ft} associated with minimal C_2Cl_4 enhancements (<5 ppt) are used in these calculations. Using Equation 1, we calculate a global BB source of 0.8± 0.4 Tg (N) y^{-1} for HCN and 0.4± 0.1 Tg (N) y^{-1} for CH_3CN. Equation 1 also leads to the conclusion that most of these emissions are due to fires (first term) and biofuels/charcoal (second term) contribute only a small fraction (10% HCN and 5% of CH_3CN) to the total BB source of cyanides.

A similar analysis was also carried out by using ERs with respect to CO. The presence of non-BB sources of CO may make these estimates somewhat less reliable. However, by using ER_{ft} values (ppt/ppb) associated with minimal C_2Cl_4 enhancements (<5 ppt), it is possible to obtain a reasonable estimate by using Equation 2.

$$[S_{HCN,CH3CN}]_{CO} = 600 \times \{14/28\} \times 10^{-3} \times \{0.74 \times ER_{ft} + 0.26 \times ER_{bl}/f\}_{CO} \qquad (2)$$

For this purpose, we adopted a global BB CO source of 600 Tg y^{-1} (74% biomass fires; 26% biofuels/charcoal) based on the most recent evaluations of BB sources [Duncan et al., 2003; Yevich and Logan, 2003]. The factor f is the CO fraction from biofuel/charcoal use in regions of eastern Asia and attempts to correct for the impact of fossil fuel CO sources on the MBL ERs. Based on the inventory developed by Streets et al. [this issue], a value of 0.55 is adopted for f. As we have seen from Equation 1, the biofuel component of HCN/CH_3CN emissions is small (<10%), so errors due to uncertainty in f are relatively modest. Using equation 2 and ERs with respect to CO from Table 1 results in a BB source estimate of 0.9± 0.4 Tg (N) y^{-1} for HCN and 0.4± 0.1 Tg (N) y^{-1} for CH_3CN, in good agreement with results from Equation 1. We caution that these estimates are relative and would be directly affected by the uncertainties in the global BB emissions of CO and CH_3Cl [Andreae and Merlet, 2001; Yevich and Logan, 2003].

In Table 4, we summarize BB source estimates of HCN and CH_3CN from published laboratory and field studies. Nearly all these estimates have been derived from measured ERs with respect to CO in controlled laboratory fires, in prescribed burns, and in real forest and savanna fires. In some instances (e. g. Lobert et al., 1991), emission factors relative to fuel nitrogen have been employed. These derived estimates typically lie in the range of 0.5-1.5 Tg (N) y^{-1} for HCN and 0.3-0.6 Tg (N) y^{-1} for CH_3CN. Recent measurements of comparatively large HCN ERs relative to CO in African fires by Yokelson et al. [2003] suggest that the HCN global BB source may be near the upper limit of this range (R. Yokelson, private communication). Our ERs, based on direct atmospheric measurements, and BB source estimates (Tables 3 and 4) are within the broad ranges that have been previously reported.

The source of variability in individual ERs in Table 3 is likely due to the dependence of ERs on the type of fuel burned and its nitrogen content. The outflow of Asian pollution represents an extremely complex mixture resulting from the heterogeneity of the fuel sources [Kato, 1996; Streets and Waldhoff, 1998]. There were instances when CO was elevated but cyanides as well as CH_3Cl were not, as may be expected from a typical industrialized urban source. There were also instances when a large elevation in CH_3Cl coexisted with little increase in CH_3CN. In a study involving a variety of burns, Yokelson et al. (1997) find that organic soils produce the highest HCN/CO, grasses are in the middle, and woody fuels produce the least amount of HCN.

3.5 Air-sea Exchange and Oceanic Sink

It is evident from Figures 3 that the atmospheric mixing ratios of HCN and CH_3CN declined towards the surface over open oceans. This is easily seen in Table 3, where statistical distribution of data filtered to remove pollution episodes (CO< 120 ppb; C_2Cl_4 <10 ppt) are summarized. All other indicators of pollution (CO, C_2H_6, C_2H_2 etc) show the opposite behavior with increasing mixing ratios near the surface. We have assessed the significance of these reduced boundary layer mixing ratios using a simple steady state box model [Singh et al., 1996]. In this model the marine boundary layer (MBL) mixing ratios are maintained by entrainment from the free troposphere and loss due to reaction with OH radicals and exchange with the ocean. As we shall see later, soils are not a likely important sink for cyanides and this gradient is mainly due to the oceanic sink.

The total flux into the MBL (F_t) was calculated by using a mean entrainment velocity (V_e) of 0.4 cm s^{-1} [Kawa and Pearson, 1989; Paluch et al., 1994; Singh et al., 1996; Faloona et al., 2003] and a concentration gradient (ΔC) across the top of the MBL derived from measurements filtered for clean atmospheric conditions (Table 3).

$$F_t = V_e \times \Delta C \quad (3)$$

To avoid biases due to scatter in the data, ΔC was determined by using median concentration differences between the free troposphere above the MBL (2-4 km) and within the MBL (0-2 km). A median gradient of 47 ppt for HCN and 20 ppt for CH_3CN from Table 2 is employed to determine F_t. A second method that normalized mixing ratios to CO was also used with comparable results. The loss in the MBL due to OH reaction (F_{OH}) was estimated by using an OH concentration of 1.5 x 10^6 molec. cm^{-3} and an MBL depth of 2 km, consistent with historic knowledge and actual observations during TRACE-P. Losses due to other radical reactions (Cl, NO_3 etc.) are small and are presently neglected. A somewhat lower MBL depth (1.5 km) did not perceptibly change results. The CH_3CN + OH rate constant ($k_{OH\text{-}CH3CN}$ = $7.8x10^{-13}$ $e^{-1050/T}$ cm^3 $molec.^{-1}$ s^{-1}) was based on the recommendation of DeMore et al [1997]. The HCN+OH rate constant ($k_{OH\text{-}HCN}$ = $1.0x10^{-13}$ $e^{-773/T}$ cm^3 $molec.^{-1}$ s^{-1} at 600 Torr) was from the recent study of Wine et al. [2002], who find this rate to be substantially slower than the DeMore et al [1997] recommendation. Although this reaction is pressure dependent, this effect is small under tropospheric conditions. A net oceanic deposition flux ($F_o = F_t - F_{OH}$) of 8.8 x 10^{-15} g (N) cm^{-2} s^{-1} and 3.4 x 10^{-15} g (N) cm^{-2} s^{-1} could be calculated for HCN and CH_3CN, respectively (Table 5).

The air-sea exchange model of Liss and Slater [1974] with newly recommended parameters [Liss and Merlivat, 1986; Nightingale et al., 2000; Donelan and Wanninkhof, 2001] was adapted to derive the under-saturation (S) necessary to maintain the oceanic deposition flux, F_o.

$$F_o = F_t - F_{OH} = K_l (C_g/H - C_l) \quad (4)$$
$$K_l = [1/k_l + 1/Hk_g]^{-1} \quad (5)$$
$$S = 1 - HC_l/C_g = H F_0/K_1 C_g \quad (6)$$
$$v_d = F_o/ C_g = S \ K_l/H \quad (7)$$

where C_l and C_g are concentrations in the bulk liquid and gas phases respectively, H (C_{sg}/C_{sl}) is the dimensionless Henry's Law constant, k_l and k_g are transfer constants for liquid and gas phases, and v_d is the corresponding deposition velocity. The temperature dependent Henry's Law constants for HCN and CH_3CN have been measured in water and best values of 3.4 x 10^{-3} (ΔH_{298} = –40.0 kj $mole^{-1}$) and 7.5 x 10^{-4} (ΔH_{298} = –50.0 kJ $mole^{-1}$), respectively were adopted for 295° K [Sander, 1999]. These were increased by 20% to correct for the salting out effect of seawater which reduces solubility [Donelan and Wanninkhof, 2001]. A liquid phase transfer constant (k_l) of 11 cm h^{-1} and a gas phase transfer constant (k_g) of 6912 $(18/MW)^{1/2}$ cm h^{-1} was used based on recommended values for a mean surface wind speed of 6 m s^{-1} [Asher, 1997; Donelan and Wanninkhof, 2001]. HCN and CH_3CN are moderately soluble in water and both liquid phase ($1/k_l$) and gas phase ($1/Hk_g$) resistances are important in controlling their air-sea flux. Using the parameters described above along with Equations 4-6, we determine that HCN and CH_3CN are under-saturated in the oceans by 27% and 6%, respectively (Table 5). An uncertainty of the order of ±20% can be placed on the calculated mean oceanic flux and under-saturation due solely to the choice of entrainment velocity.

Based on the present observations, a deposition velocity (v_d) of 0.12 cm s^{-1} for HCN and 0.06 cm s^{-1} for CH_3CN is calculated from equation 7. These values are appropriate for deposition

over open oceans. Using a different set of assumptions, Li et al [this issue] find that a v_d of 0.13 cm s^{-1} for both HCN and CH_3CN provides a reasonable fit to the present data. We were unable to uncover independent studies of HCN dry deposition. However, several estimates of CH_3CN deposition velocity have been made [De laat et al., 2001; De Gouw et al., 2003, Karl et al., 2003]. These estimates have been typically in the range of 0.01 to 0.2 cm s^{-1}. In a recent study performed in the upwelling south Atlantic regions off of the Namibian and Angolan coasts, Jost et al. [2003] find that a much higher dry deposition velocity of the order of 0.4 cm s^{-1} best fits their observations. It is possible that deposition velocities over coastal regions are larger than over open oceans. Clearly additional HCN and CH_3CN studies are needed for an accurate assessment of the oceanic sink.

For seawater under-saturation to persist, a removal mechanism within the oceans is necessary. Chemical reaction pathways for HCN and CH_3CN degradation (e. g. hydrolysis, Cl^-) are too slow to be a significant process. In polluted streams bio-remediation of HCN has been a common industrial practice. Enzymatic reactions in aerobic conditions can relatively quickly deplete HCN to ammonia {$HCN+1/2O_2 \rightarrow HOCN (+ H_2O) \rightarrow NH_3+CO_2$}. Similar removal is also known to occur for CH_3CN. In one study of river streams, unaided biodegradation was sufficient to remove these cyanides with a half-life of about two weeks [EPA, 1985; 1992]. By analogy, we believe that oceanic removal via biological degradation is a likely possibility. Although bacteria present in soils could also destroy cyanides, there is no evidence to support that this is an important loss mechanism in part because cyanides are rapidly and preferentially exchanged to the air medium. It should be noted that the presence of a net sink does not imply that there are no additional oceanic sources. These sources, if present, could be masked by the oceanic degradation. We were unable to find any direct seawater observations to confirm the hypothesis of under-saturation or to ascertain the rate of loss of HCN and CH_3CN.

3.6 Atmospheric Lifetimes and Global Budgets

Development of an accurate global budget for HCN and CH_3CN requires far more extensive observational data than is currently available. As a first step, we attempt to use our measurements over the Pacific for this purpose by relying on reasonable extrapolations and assumptions. We extrapolate the TRACE-P observations of HCN and CH_3CN in time and space by scaling them to the seasonal and latitudinal profile of the column of HCN which has been extensively derived from spectroscopic observations and also modeled [Zhao et al., 2000, 2002; Notholt et al., 2000; Li et al., 2000; Rinsland et al., 2001; 2002]. In the absence of direct observations and given the presumed commonality of sources, we consider this extrapolation to be a reasonable first step for both HCN and CH_3CN. The seasonal cycle of HCN reported by Zhao et al. [2000] over Japan indicated that the annual average mixing ratios at mid-latitudes are 1.08 times those in spring. Latitudinal extrapolation to the globe, based on Notholt et al. [2000] and Rinsland et al. [2002], resulted in a scaling factor of 0.92. Fortuitously, these two factors (seasonal and latitudinal) result in a net scaling factor of 1.0. Thus the springtime mid-latitude measurements of HCN made during TRACE-P closely resemble the global annual average. For extrapolation to global scales, median concentrations under relatively clean conditions (Table 2) are utilized. We also assume that the oceanic fluxes estimated for the TRACE-P region are representative of global oceans.

Table 5 summarizes the global budget of HCN and CH_3CN based on the present observations and noted assumption. The calculated oceanic deposition flux is equivalent to a deposition of 1.0 Tg (N) y^{-1} of HCN and 0.4 Tg (N) y^{-1} of CH_3CN to the global oceans. This

nitrogen deposition of 1.4 Tg (N) y^{-1} is only a small fraction of the total nitrogen deposition into the oceans of 30 Tg (N) y^{-1} (Duce, 1998). However, this nearly uniform global nutrient source may still play an important role in remote oceans. The total annual tropospheric burden of HCN and CH_3CN is determined to be 0.44 Tg (N) and 0.30 Tg (N), respectively. The oceanic removal rate thus corresponds to an atmospheric residence time of 5.3 months for HCN and 9.2 months for CH_3CN. Using the OH reaction rates (in units of cm^3 $molec.^{-1}$ s^{-1}) noted earlier ($k_{OH\text{-}CH3CN} = 7.8x10^{-13}\ e^{-1050/T}$; $k_{OH\text{-}HCN} = 1.0x10^{-13}\ e^{-773/T}$) and a CH_3CCl_3 lifetime of 5 years corresponding to a global mean OH of ≈1 x 10^6 molec. cm^{-3}. [Montzka et al., 2000], we derive a mean residence time of 63 months for HCN and 23 months for CH_3CN due to removal by reaction with OH radicals. We note that this HCN residence time is nearly 4 times larger that inferred from the DeMore et al., [1997] recommendation. Clearly there is much uncertainty associated with these OH rate constants. Given the extremely low solubility of these cyanides, we expect removal by processes such as rain out and wash out to be unimportant in comparison [Crutzen and Lawrence, 2000]. Loss due to reactions with Cl, $O(^1D)$, and NO_3 radicals is calculated to be negligibly small. Although soil bacteria could destroy cyanides, limited studies have shown that cyanides are quickly released after deposition to soil and this sink [EPA 1985; 1992], although poorly studied, is expected to be minor. The mean atmospheric residence time, based on OH and oceanic loss, is 5.0 months for HCN and 6.6 months for CH_3CN (Table 5). The calculated burden and residence times imply that a global source of some 1.1 Tg (N) y^{-1} for HCN and 0.5 Tg (N) y^{-1} for CH_3CN is present. The 5 month mean lifetime of HCN can be compared with a range of 2-4 months derived by Li et al. (2000). Similarly, the 7 month lifetime of CH_3CN can be compared with estimates of 3-11 months by Hamm and Warneck [1990], 1 month by Bange and Williams [2000], and approximately 5 months by Karl et al. [2003].

It is evident from Tables 3 and 5 that our estimates of the BB sources can account for most of the needed source for HCN and CH_3CN. Nevertheless the possibility of additional sources is not ruled out. According to the Toxics Release Inventory of US EPA (http://www.epa.gov/tri), the 1999 total U. S. emissions for HCN and CH_3CN were 1.6 x 10^9 g (N) y^{-1} (55% air discharge) and 3.2 x 10^9 g (N) y^{-1} (5% air discharge), respectively. Thus direct industrial releases of HCN and CH_3CN are extremely small (<0.02 Tg (N) y^{-1}). Measurements over urban Los Angeles during TRACE-P (Mission 20 and test flights) along with the direct measurements of CH_3CN in automobile exhaust by Holzinger et al., [2001] are consistent with the view that fossil fuel combustion is a miniscule source (<0.02 Tg (N) y^{-1}). We note here that cyanides are easily formed during processes of high temperature fuel combustion ($CH + N_2 \rightarrow HCN + N$) but are instantly converted to NO resulting in nearly zero net emissions. There is also the possibility that biogenic sources of HCN (and CH_3CN) may be present. In several studies cut leaves are found to have significant levels of HCN (1 mg/g dry weight). High amounts of cyanogenic glycosides (1-30 mg/kg), which are quickly converted to HCN upon maceration, are found in common foods such as almonds and Lima beans. A mechanism for the formation and release of HCN from linamarin (a cyanogenic glycoside) has been discussed by Fall et al., [2001]. Tyndall et al. [2001] also suggest that CH_3CN oxidation by OH could also yield some HCN. The budget analysis presented in Table 5 does not rule out the possibility that primary biogenic or secondary sources of <0.2 Tg (N) y^{-1} may be present.

The budget presented in Table 5 must be considered a somewhat rough estimate in large part because of the extreme paucity of available data. Many of the assumptions and extrapolations (e. g. uniform oceanic under-saturation) have not yet been tested in varied geographical locations and seasons. We should expect losses in coastal, open, and upwelling

oceanic regions to vary. Detailed studies of soil deposition and loss have not been performed. At the present time, there is insufficient data to quantify the uncertainties associated with estimates in Table 5. Substantial additional atmospheric and oceanic data are required to refine these estimates.

4. Conclusions

In-situ measurements of HCN and CH_3CN are consistent with the view that biomass burning is the largest source and oceanic loss the largest sink. The global budget of these cyanides is in rough balance but the possibility of small additional sources and sinks is not ruled out. While these chemicals are convenient tracers of biomass burning pollution, their atmospheric and biogeochemical cycles are poorly understood. There is little in-situ data currently available on the atmospheric distribution of cyanides from the Northern Hemisphere and virtually none from the Southern Hemisphere. The paucity of oceanic data is even more glaring. While bacterial loss in the oceans is postulated as the main loss process, no chemical or biological data from the oceans is currently available. The assumption that soils are a minor sink is poorly validated. There is a need to better quantify the global budget of cyanides including a better mechanistic understanding of combustion sources and biological sinks. The potential of upcoming satellite instruments to measure of HCN and possibly CH_3CN in the troposphere hold great promise.

Acknowledgments: This research was funded by the NASA Global Tropospheric Experiment. We thank all TRACE-P participants for their support. Comments and suggestions by R. Yokelson of the University of Montana are much appreciated.

References

Andreae, M. O. et al., Transport of biomass burning smoke to the upper troposphere by deep convection in the equatorial region, Geophy. Res. Lett., 28, 951–954, 2001.

Andreae, M. O. and P. Merlet, Emissions of trace gases and aerosols from biomass burning, Global Biogeochem. Cycles , 15 (4), 955-966, 2001.

Arnold, F. H., H. Bohringer, and G. Henschen, Composition measurements of stratospheric positive ions, Geophys. Res. Lett., 5, 653–656, 1978.

Asher, N. V., The sea-surface microlayer and its effect on global air-sea gas transfer, in *The sea surface and global change*, edited by P. S. Liss and R. A. Duce, pp 251-285, Cambridge University Press, Cambridge, 1997.

Bange, H. W. and J. Williams, New directions: acetonitrile in atmospheric and biogeochemical cycles, Atmos. Environ., 34, 4959-4960, 2000.

Becker, K.H., and A. Ionescu, Acetonitrile in the lower atmosphere, Geophy. Res. Lett., 9, 1349 – 1351, 1982.

Butler, J. H., Better budgets for methyl halides?, Nature, 403, 260-261, 2000.

Cicerone, R. J., and R. Zellner, The atmospheric chemistry of hydrogen cyanide (HCN), J. Geophys. Res., 88, 10689 - 10696, 1983.

Coffey, M. T., W. G. Mankin, and R. J. Cicerone, Spectroscopic detection of stratospheric hydrogen cyanide, Science, 214, 333 - 334, 1981.

Crutzen, P. J., et al., High spatial and temporal resolution measurements of primary organics and their oxidation products over the tropical forests of Surinam, Atmos. Environ., 34, 1161-1165, 2000.

Crutzen, P. J., and M. G. Lawrence, Impact of precipitation scavenging on the transport of trace gases: A 3-dimensional model sensitivity study, J. Atmos. Chem., 37, 81-112, 2000.

de Gouw, J. A., C. Warneke, D. D. Parrish, J. S. Holloway, M. Trainer, and F. C. Fehsenfeld, Emission sources and ocean uptake of acetonitrile (CH_3CN) in the atmosphere, J. Geophys. Res., submitted, 2003.

de Laat, A. T. J., J. A. de Gouw, J. Lelieveld, and A. Hansel, Model analysis of trace gas measurements and pollution impact during INDOEX, J. Geophys. Res., 106, 28,469-28,480, 2001.

DeMore, W. B., Sander, S. P., Golden, D. Hampson, R. F., Kurylo, M. J., Howard, C. J., Ravishankara, A. R., C. E. Kolb, and Molina, M. J., Chemical kinetics and photochemical data for use in stratospheric modeling, Evaluation No. 12, 1997.

Donelan, M.A., and R. Wanninkhof, Gas Transfer at Water Surfaces- concepts and issues, in *Gas Transfer at Water Surfaces*, edited by M. Donelan, W. Drennan, E. Saltzman, and R. Wanninkhof, pp. 1-10, AGU, Geophysical Monograph 127, Washington, 2001.

Duce, R. A., The input of atmospheric chemicals to the ocean, WMO Bulletin 47, 51-60, 1998.

Duncan, B. N., R. V. Martin, A. C. Staudt, R. Yevich, and J. A. Logan, Interannual and seasonal variability of biomass burning emissions constrained by satellite observations, J. Geophys. Res., 108(D2), 4040, doi:10.1029/2002JD002378, 2003.

EPA, Health and environmental effects profile for acetonitrile, US EPA, Washington, D. C., ECAO-CIN-P137, 1985.

EPA, Drinking water criteria document for cyanides, US EPA, Washington, D. C., PB92-173319, 1992.

Fall, R., T. G. Custer, S. Kato, and V. M. Bierbaum, New directions: the biogenic acetone-HCN connection, Atmos. Environ., 35, 1713-1714, 2001.

Faloona, I., D. Lenschow, T. Campos, B. Stevens, B. Blomquist, D. Thornton, A. Bandy, and H. Gerber.Observations of entrainment in eastern Pacific marine stratocumulus using three conserved scalars, J. of Atmos. Sci., submitted, 2003.

Hamm, S. and P. Warneck, The interhemispheric distribution and the budget of acetonitrile in the troposphere, J. Geophys. Res., 95, 20,593-20,606, 1990.

Holzinger, R., C. Warneke, A. Hansel, A. Jordan, W. Lindinger, D. H. Scharffe, G. Schade, P. J. Crutzen, Biomass burning as a source of formaldehyde, acetaldehyde, methanol, acetone, acetonitrile, and hydrogen cyanide, Geophys. Res. Lett., 26, 1161-1164, 1999.

Holzinger, R. C., A. Jordan, A. Hansel, and W. Lindinger, Automobile emissions of acetonitrile: assessment of its contribution to the global source, J. Atmos. Chem., 38, 187-193, 2001.

Jacob, D. J. et al., An overview of the NASA GTE/TRACE-P mission-spring 2001, J. Geophys. Res, this issue.

Jost, C., J. Trentmann, D. Sprung, M. O. Andreae, and K. Dewey, Deposition of acetonitrile over the Atlantic Ocean near Namibia and Angola, Geophys. Res. Lett., in preparation, 2003.

Karl, T., Hansel A., Maerk, T., Lindinger, W., and D. Hoffman, Trace Gas Monitoring at the Mauna Loa Baseline Observatory using Proton Transfer Reaction Mass Spectrometry, Int. Journal for Mass Spectrometry, 223/224, 527-538, 2003.

Kato, N., An analysis of the structure of energy consumption and dynamics of emissions of atmospheric species related to the global environmental change (SO_2, NO_x, and CO_2), Atmos. Environ., 30, 757-785, 1996.

Kawa, S. R., and R. Pearson, Jr., Ozone budgets from the Dynamics and Chemistry of Marine Stratocumulus Experiment, J. Geophys. Res., 94, 9809-9817, 1989.

Lelieveld, J. et al., The Indian Ocean Experiment: Widespread air pollution from south and south east Asia, Science, 291, 1031-1036, 2000.

Li, Q., D. J. Jacob, I. Bey, R. M. Yantosca, Y. Zhao, Y. Kondo, and J. Notholt, Atmospheric hydrogen cyanide (HCN): biomass burning source, oceanic sink? Geophys. Res. Lett., 27, 357-360, 2000.

Li, Q., D. J. Jacob, I. Bey, R. M. Yantosca, C. L. Heald, H. B. Singh, M. Koike, Y. Zhao, G. Sachse, D. G. Streets, A global 3-D model evaluation of the atmospheric budget of HCN and CH_3CN: Constraints from aircraft measurements over the western Pacific, J. Geophys. Res, this issue.

Liss, P. S. and P. G. Slater, Flux of gases across the air-sea interface, Nature, 247, 181-184, 1974.

Liss, P. S. and L. Merlivat, Air sea gas exchange rates: Introduction and synthesis, in *The role of air-sea exchange in geochemical cycling*, Ed. P. Buart-Menard, 113-129, Reidel, Boston, 1986.

Livesey, N. J., R. Zellner, J. W. Waters, R. Khosravi, G. P. Brasseur, G. S. Tyndall, and W. G. Reed, Stratospheric CH_3CN from the UARS microwave limb sounder, Geophys. Res. Lett., 28, 779 – 782, 2001.

Lobert, J. M., D. H. Scharffe, W. M. Hao, P. J. Crutzen, Importance of biomass burning in the atmospheric budgets of nitrogen-containing gases, Nature, 346, 552-554, 1990.

Lobert, J. M., Scharffe, D. H., Kuhlbusch, T. A., Seuwen, R., and Crutzen, P. J., Experimental evaluation of biomass burning emissions: nitrogen and carbon containing compounds, Global Biomass Burning, J. S. Levine (eds), MIT Press, 289-304, 1991.

Lobert, J. M., W. C. Keene, J. A. Logan, and, R. Yevich, Global chlorine emissions from biomass burning: Reactive chlorine emissions inventory, J. Geophys. Res., 104, 8373-8389, 1999.

Mahieu, E., C. P. Rinsland, R. Zander, P. Demoulin, L. Delbouille, G. Roland, Vertical column abundances of HCN deduced from ground-based infrared solar spectra: Long-term trend and variability, J. Atmos. Chem., 20, 299-310 1995.

Mahieu, E., R. Zander, L. Delbouille, P. Demoulin, G. Rolands, and S. Servais: Observed trends in total vertical column abundances of atmospheric bases for IR solar spectra recorded at the Jungfraujoch, J. Atmos. Sci., 29, 227-243, 1997.

Montzka, S. A., C. M. Spivakovsky, J. H. Butler, J. W. Elkins, L. T. Lock and D. J. Mondeel, New observational constraints for atmospheric hydroxyl on global and hemispheric scales, Science, 288, 500 - 503, 2000.

Notholt, J., Toon, G. C., Rinsland, C. P., Pougatchev, N. S., Jones, N. B., Connor, B. J., Weller, R., Gautrois, M., Schrems, O., Latitudinal variations of trace gas concentrations in the

free troposphere measured by solar absorption spectroscopy during a ship cruise, J. Geophys. Res., 105, 1337-1349, 2000.

Nightingale, P. D., Malin, G., Law, C. S. Watson, A. J., Liss, P. S., Liddicoat, M. I., Boutin, J., Upstill-Goddard, R. C., In situ evaluation of air-sea gas exchange parameterizations using novel conservative and volatile tracers, Global Biogeochem. Cycles, 14, 373-388, 2000.

Paluch, I.R., D.H. Lenschow, S. Siems, G.L. Kok, and R.D. Schillawski, Evolution of the subtropical marine boundary layer, Part I: Comparison of soundings over the eastern Pacific from FIRE and HaRP, J. Atmos. Sc., 51, 1465-1479, 1994.

Reiner, T., Sprung, D., Jost, C., Gabriel, R., Mayol-Bracero, O. L., Andreae, M. O., Campos, T. L., Shetter, R. E., Chemical characterization of pollution layers over the tropical Indian Ocean: Signatures of emissions from biomass and fossil fuel burning, J. Geophys. Res., 106 , 28,497- 28,510, 2001.

Rinsland, C. P., et al., ATMOS/ATLAS 3 infared profile measurements of trace gases in the November 1994 tropical and subtropical troposphere, J. Quant. Spectrosc. Radiat. Transfer, 60, 891-901, 1998.

Rinsland, C.P., et al., Infrared solar spectroscopic measurements of free tropospheric CO, C_2H_6, and HCN above Mauna Loa, Hawaii: Seasonal variations and evidence for enhanced emissions from the southeast Asian tropical fires of 1997-1998, J. Geophys. Res., 104, 18667-18680, 1999.

Rinsland, C.P., E. Mahieu, R. Zander, P. Demoulin, J. Forrer, and B. Buchmann, Free tropospheric CO, C_2H_6, and HCN above central Europe: Recent measurements from the Jungfraujoch station including the detection of elevated columns during 1998, J. Geophys. Res., 105, 24235-24249, 2000.

Rinsland, Curtis P.; Meier, A.; Griffith, D.; Chiou, L. S., Ground-based measurements of tropospheric CO, C_2H_6, and HCN from Australia at 34*S latitude during 1997-1998**,** J. Geophys. Res.**,** 106 **,** D18, 20,913-20,924**,** 2001.

Rinsland, C. P.; Jones, N. B.; Connor, B. J.; Wood, S. W.; Goldman, A.; Stephen, T. M.; Murcray, F. J.; Chiou, L. S.; Zander, R.; Mahieu, E., Multiyear infrared solar spectroscopic measurements of HCN, CO, C_2H_6, and C_2H_2 tropospheric columns above Lauder, New Zealand (45°S latitude)**,** J. Geophys. Res.**,** 107**,** D14**,** ACH 1-1 to ACH 1-12, 2001JD001150, 2002

Sander, R, Compilation of Henry's law constants for inorganic and organic species of potential importance in environmental chemistry, http://www.mpch-mainz.mpg.de/~sander/res/henry.html, version 3, 1999.

Schneider, J., Bürger, V., Arnold, F., Methyl cyanide and hydrogen cyanide measurements in the lower stratosphere: Implications for methyl cyanide sources and sinks, J. Geophys. Res., 102, 25,501-25,506, 1997.

Singh, H. B. et al., Low ozone in the marine boundary layer of the tropical Pacific Ocean: photochemical loss, chlorine atoms, and entrainment, J. Geophys. Res., 101, 1907-1918, 1996.

Singh, H. B. and D. J. Jacob, Future directions: Satellite observations of tropospheric Chemistry, Atmos. Environ, 34, 4399-4401, 2000.

Singh, H, Y. Chen, A Staudt, D. Jacob, D. Blake, B. Heikes, J. Snow. Evidence from the Pacific troposphere for large global sources of oxygenated organic compounds. Nature, 410, 1078-1081, 2001.

Snider, J. and G. Dawson, Surface acetonitrile near Tucson, Arizona, Geophys. Res. Lett., 11, 241 – 242, 1984.

Streets, D. G. and S. T. Waldhoff, Biofuel use in Asia and acidifying emissions, Energy, 23, 1029-1042, 1998.

Streets, D.G., et al., A year-2000 inventory of gaseous and primary aerosol emissions in Asia to support TRACE-P modeling and analysis, J. Geophys. Res, this isue.

Tyndall, G. S., J. J. Orlando, T. J. Wallington, and M. D. Hurley, Products of the Chlorine-Atom- and Hydroxyl-Radical-Initiated Oxidation of CH_3CN, J. Phys. Chem. A, 105, 5380–5384, 2001.

Verschueren, K., Handbook of environmental data on organic chemicals, 3rd Edition, Van Nostrand Reinhold, New York, 1996.

Williams, J., U. Pöschl, P. J. Crutzen, A. Hansel, R. Holzinger, C. Warneke, W. Lindinger, and J. Lelieveld, An atmospheric chemistry interpretation of mass scans obtained from a Proton Transfer Mass Spectrometer flown over the tropical rainforest of Surinam, J. of Atmos. Chem., 38, 133-166, 2001.

Wine, P. H., R. S. Strekowski, J. Nicovich, M. L. McKee, G. Chen, and D. D. Davis, Atmospheric Chemistry of HCN, paper PHYS 134, presented at the 224th ACS National Meeting, Boston, MA, 2002.

Wisthaler, A., A. Hansel, R. R. Dickerson, and P. J. Crutzen, Organic trace gas measurements by PTR-MS during INDOEX 1999, J. Geophys. Res., 107 (D19), 8024, doi:10.1029/2001JD000576, 2002.

Yevich, R. and J. A. Logan, An assessment of biofuel use and burning agricultural waste in the developing world, Global Biogeochem. Cycles, in press, 2003.

Yokelson, R. J., D. E. Ward, R. A. Susott, J. Reardon, and D. W. T. Griffith, Emissions from smoldering combustion of biomass measured by open-path Fourier transform infrared spectroscopy, J. Geophys. Res., 102, 18,865-18,877, 1997.

Yokelson, R. J., I. Bertschi, T. C. Christian, P. V. Hobbs, D. E. Ward, W. M. Hao, An overview of trace gas measurements in nascent, aged, and cloud-processed smoke from African savanna fires by airborne Fourier transform infrared spectroscopy (AFTIR), S2K special issue, submitted, 2003.

Zhao, Y., Y. Kondo, F. J. Murcray, X. Liu, M. Koike, H. Irie, K. Strong, K. Suzuki, M. Sera, and Y. Ikegami, Seasonal variations of HCN over Northern Japan measured by ground-based infrared solar spectroscopy, Geophys. Res. Lett., 27, 2085-2088, 2000.

Zhao, Y.; Strong, K.; Kondo, Y.; Koike, M.; Matsumi, Y.; Irie, H.; Rinsland, C. P.; Jones, N. B.; Suzuki, K.; Nakajima, H.; Nakane, H.; Murata, I., Spectroscopic measurements of tropospheric CO, C_2H_6, C_2H_2, and HCN in northern Japan, J. Geophys. Res., 107, D18, 10.1029/2001JD000748, 2002.

Table 1: Atmospheric mixing ratios of HCN, CH_3CN, and selected tracers in the Pacific troposphere based on all TRACE-P tropospheric data

Altitude (km)	HCN (ppt)	CH_3CN (ppt)	CO (ppb)	CH_3Cl (ppt)	C_2Cl_4 (ppt)
0-2	233.5 ± 160.6 (196.6, 244)*	115.3 ± 50.7 (105.6, 242)	194.2 ± 88.8 (173.5, 428)	580.7 ± 101.3 (554.3, 393)	10.2 ± 8.9 (9.2, 393)
2-4	248.2 ± 116.7 (208.9, 156)	148.4 ± 65.1 (128.7, 175)	150.8 ± 54.6 (131.0, 281)	572.9 ± 37.4 (559.2, 264)	6.6 ± 6.0 (5.5, 264)
4-6	243.8 ± 70.3 (226.3, 94)	146.4 ± 47.5 (137.4, 125)	130.6 ± 46.3 (116.3, 218)	565.1 ± 26.0 (556.9, 203)	5.3 ± 3.5 (4.4, 200)
6-8	246.6 ± 66.1 (232.0, 99)	153.2 ± 43.6 (142.5, 144)	118.9 ± 40.3 (110.6, 229)	564.7 ± 28.6 (559.1, 220)	4.1 ± 2.3 (3.6, 220)
8-10	254.0 ± 91.6 (225.3, 108)	177.9 ± 48.7 (162.7, 201)	122.1 ± 42.8 (108.9, 308)	580.0 ± 32.0 (578.0, 293)	3.2 ± 1.5 (2.7, 288)
10-12	235.9 ± 77.0 (227.6, 45)	166.0 ± 49.1 (152.7, 128)	102.0 ± 35.8 (85.8, 206)	573.5 ± 31.8 (569.0, 200)	2.2 ± 1.1 (2.1, 199)
0-12	242.7 ± 118.4 (218.4, 746)	149.0 ± 55.9 (138.0, 1015)	143.6 ± 67.7 (127.2, 1670)	574.1 ± 57.9 (561.0, 1573)	5.8 ± 6.1 (4.4, 1564)

* Mean ± 1 standard deviation (median, number of data points)

Table 2: Atmospheric mixing ratios of HCN, CH_3CN, and selected tracers in the Pacific troposphere under relatively unpolluted conditions (CO<120 ppb or C_2Cl_4<10 ppt)

Altitude (km)	HCN (ppt)	CH_3CN (ppt)	CO (ppb)	CH_3Cl (ppt)	C_2Cl_4 (ppt)
0-2	161.8 ± 58.3 (130.0, 21)*	125.5 ± 24.8 (112.7, 21)	103.9 ± 8.6 (104.9, 40)	548.7 ± 11.5 (546.3, 34)	4.0 ± 0.8 (3.9, 34)
2-4	187.0 ± 65.2 (177.2, 51)	136.7 ± 30.7 (133.1, 57)	103.9 ± 12.0 (106.6, 87)	554.4 ± 20.2 (550.0, 81)	4.1 ± 1.4 (4.2, 81)
4-6	220.7 ± 53.3 (202.3, 46)	147.9 ± 30.8 (140.7, 67)	99.8 ± 13.1 (102.0, 118)	555.3 ± 14.3 (552.4, 114)	3.4 ± 1.2 (3.2, 111)
6-8	217.0 ± 41.4 (217.5, 59)	142.3 ± 25.3 (138.3, 96)	98.3 ± 14.8 (99.6, 157)	555.1 ± 19.0 (555.0, 149)	3.1 ± 1.3 (2.7, 149)
8-10	213.9 ± 35.8 (214.3, 61)	154.3 ± 28.9 (148.4, 125)	95.5 ± 13.5 (96.8, 191)	563.3 + 22.5 (567.0, 179)	2.5 ± 1.0 (2.2, 174)
10-12	228.1 ± 52.2 (227.6, 21)	144.7 ± 33.8 (136.3, 89)	83.0 ± 12.5 (80.9, 151)	558.7 ± 20.7 (554.0, 146)	1.8 ± 0.8 (1.8, 145)
0-12	207.5 ± 53.2 (207.9, 259)	145.4 ± 30.3 (141.6, 455)	95.7 ± 14.8 (96.4, 744)	557.6 ± 19.9 (555.0, 703)	2.9 ± 1.3 (2.5, 694)

* Mean ± 1 standard deviation (median, number of data points)

Table 3: Enhancement Ratios (ERs) of HCN and CH_3CN with respect to CO and CH_3Cl in selected plumes in the free troposphere (3-12 km; ER_{ft}) and in pollution episodes in the marine boundary layer (0-1 km; ER_{bl})

Flight No.	Lat. (˚N)	Long (˚E)*.	Altitude (km)	ΔC_2Cl_4 (ppt)	$\Delta CH_3CN/\Delta CH_3Cl$ (ppt/ppt)	$\Delta HCN/\Delta CH_3Cl$ (ppt/ppt)	$\Delta CH_3CN/\Delta CO$ (ppt/ppb)	$\Delta HCN/\Delta CO$ (ppt/ppb)	Comments
4	40.1	-132.0	6-10	4	1.38	2.46	1.37	2.31	

4	31.9	-150.8	6-10	0	1.00	1.42	1.62	2.31	
5	17.9	-177.0	3	8	1.63	2.36	1.44	2.08	
5	17.4	171.0	3	2	1.65	3.34	1.36	2.75	
7	30.5	128.0	6-7	11	1.41	1.93	0.95	1.30	
8	22.8	140.5	4-6	10	1.60	1.20	1.00	0.75	
14	22.5	143.8	9	3	1.85	ND*	1.00	ND	
17	33.7	149.5	4-5	8	0.50	2.80	0.26	1.47	
18	35.4	148.0	10	2	1.90	ND	1.90	ND	
18	33.4	166.7	10	1	1.62	3.38	1.85	3.85	
18	28.2	-177.4	9-10	3	1.95	3.18	1.79	2.91	
19	36.0	-137.5	8-9	0	2.46	6.62	2.78	6.32	
Mean $ER_{ft} \pm 1\sigma$ (3-12 km, all data)					1.58±0.49	2.86±1.52	1.44±0.63	2.60±1.57	
Mean $ER_{ft} \pm 1\sigma$ (3-12 km, ΔC_2Cl_4 <5ppt)					1.73±0.43	3.40±1.74	1.71±0.53	3.41±1.53	
6	27.6	125.0	0.3	11	NM	NM	0.00	0.50	$\Delta CH_3Cl=\Delta CH_3CN=$ 0 ppt
6	18.9	119.3	0-1	12	0.83	2.60	0.50	1.56	
8	20.5	125.5	0.3	10	1.54	3.38	1.18	2.58	
9	32.5	124.9	0-1	10	0.00	4.00	0.00	1.86	
9	33.8	124.8	1.0	10	0.00	2.97	0.00	2.01	
10	21.6	129.7	0.3	8	NM	NM	0.00	0.00	$\Delta CH_3Cl=\Delta HCN=\Delta CH_3CN=$ 0; $\Delta CO=$86 ppb
12	24.6	120.6	0.3	28	0.19	0.21	0.33	0.38	$\Delta CH_3CN=$ 0 ppt; coastal Chinese sources
13	28.9	125.1	0.3	118	0.19	1.33	0.25	1.71	Shanghai plume
16	28.3	124.9	1.0	8	0.00	2.86	0.00	1.26	$\Delta CH_3CN=$ 0 ppt
Mean $ER_{bl} \pm 1\sigma$ (0-1 km, all data)					0.40±0.58	2.48±1.29	0.25±0.40	1.32±0.86	

*ND - no data; Negative sign denotes °W, NM – not measurable

Table 4: Estimates of the global biomass burning (BB) source of HCN and CH_3CN*

HCN Global BB source - Tg(N) y^{-1}	CH_3CN Global BB source - Tg(N) y^{-1}	Type of measurement	Source
1.5 (0.6-3.2)	0.6 (0.2-1.1)	Controlled laboratory fires	Lobert et al. [1990; 1991]
0.4 ± 0.2	0.5 ± 0.3	Controlled laboratory fires	Holzinger et al. [1999]
--	0.3	Literature review and assessment	Bange and Williams [2000]

--	0.4	Plumes over Surinam	Andreae et al. [2001]
--	0.4-1.2	Plumes over the Indian Ocean	Reiner et al. [2001]
0.5	0.4	Literature review and assessment	Andreae and Merlet [2001]
0.9 ± 0.4**	0.4 ± 0.1**	Plumes over the Pacific	This study (data normalized to CO)
0.8 ± 0.4**	0.4 ± 0.1**	Plumes over the Pacific	This study (data normalized to CH_3Cl)

* Sources are generally derived from measured Emission Ratios (ERs) with respect to CO in controlled laboratory fires, in prescribed burns, and in real forest and savanna fires.
** Derived from mean ERs in Table 3 based on a global BB source of 600 Tg y^{-1} for CO and 0.9 Tg y^{-1} for CH_3Cl. It is assumed that Enhancement Ratios are effectively the same as Emission Ratios. See text for details.

Table 5: An estimate of the mean atmospheric lifetime and global budget of HCN and CH_3CN

Parameters	HCN	CH_3CN
Median gradient between free troposphere (2-4 km) and MBL (0-2 km) from Table 2	47 ppt	20 ppt
Calculated oceanic deposition flux (F_o)*	8.8 x 10^{-15} g (N) cm^{-2} s^{-1}	3.4 x 10^{-15} g (N) cm^{-2} s^{-1}
Oceanic under-saturation**	27%	6%
Deposition velocity (v_d) for open ocean**	0.12 cm s^{-1}	0.06 cm s^{-1}
Global loss to oceans[#]	1.0 Tg (N) y^{-1}	0.4 Tg (N) y^{-1}
Annual mean atmospheric burden[#]	0.44 Tg (N)	0.30 Tg (N)
Residence time due to OH reaction[$]	63 months	23 months
Residence time due to oceanic sink[#]	5.3 months	9.2 months
Global mean residence time	5.0 months	6.6 months
Calculated global source	1.1 Tg (N) y^{-1}	0.5 Tg (N) y^{-1}
Mean biomass burning source from this study	0.8 Tg (N) y^{-1}	0.4 Tg (N) y^{-1}

Anthropogenic (industrial/fossil fuel) sources	<0.05 Tg (N) y^{-1}	<0.05 Tg (N) y^{-1}
Biogenic/other sources (by difference)	0-0.2 Tg (N) y^{-1}	0-0.1 Tg (N) y^{-1}

*Based on a mean entrainment velocity of 0.4 cm s^{-1} and an OH value of $1.5x10^6$ molec. cm^{-3} in MBL (0-2 km).
**Calculated using an air-sea exchange model (see text for detail).
[#] Extrapolations to the globe are carried out by scaling to the seasonal and latitudinal behavior of the remotely sensed total column of HCN (see text for detail).
[$] Calculated by normalizing to a CH_3CCl_3 lifetime of 5 years (OH ≈ 1 x 10^6 molec. cm-^{3}).

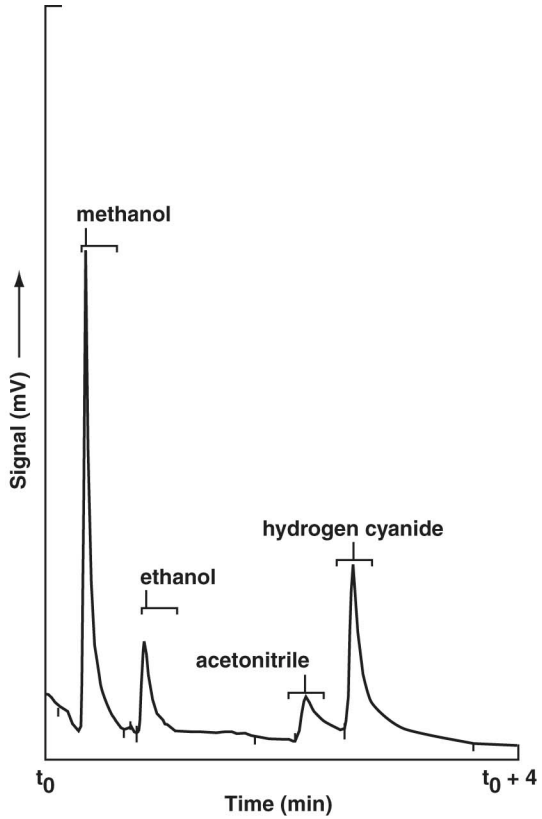

Figure 1: A sample chromatogram of the atmospheric detection of HCN and CH_3CN using a Reduction Gas Detector (RGD). Sample size is 200 ml.

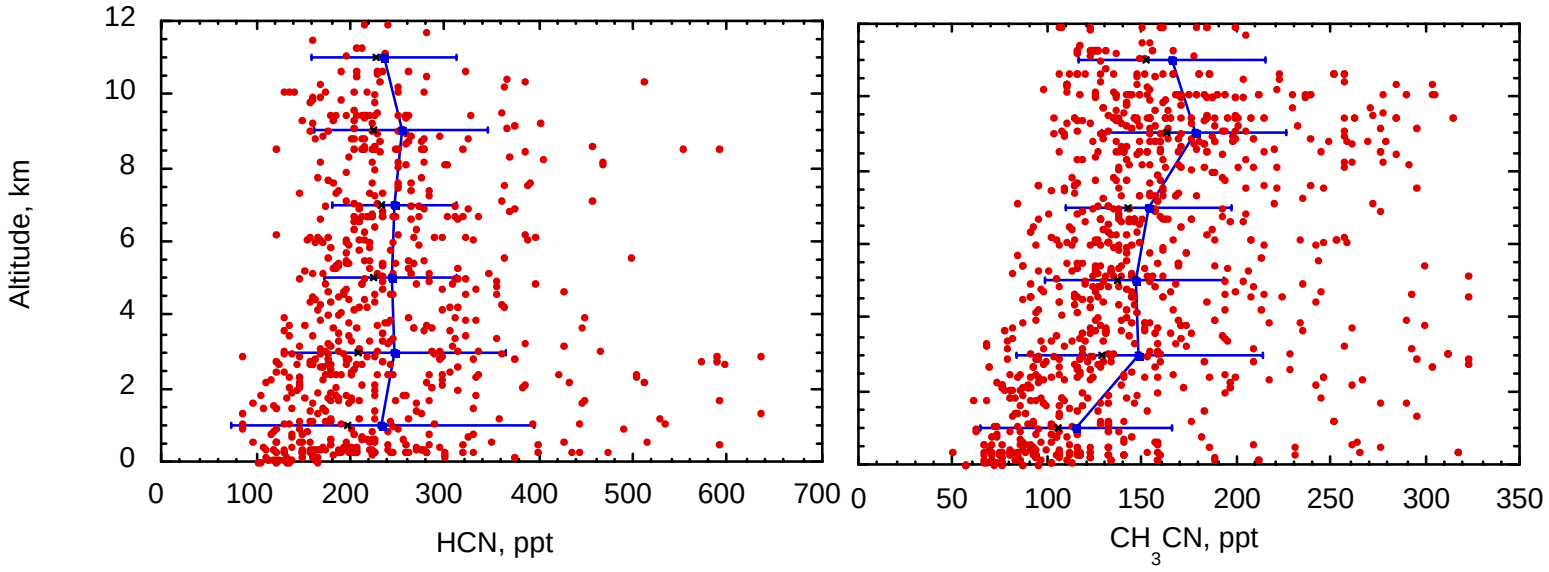

Figure 2: Vertical structure of HCN and CH_3CN over the Pacific as measured during TRACE-P

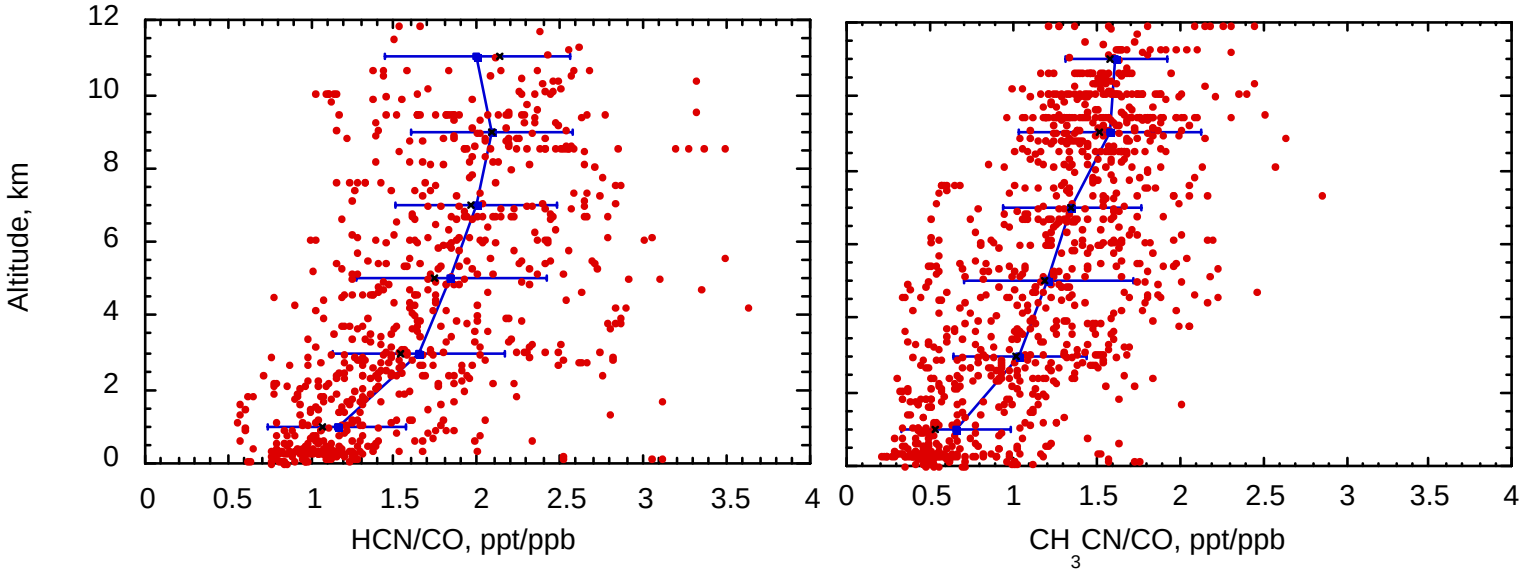

Figure 3: Vertical structure of the relative abundance of HCN and CH_3CN with respect to CO in the troposphere

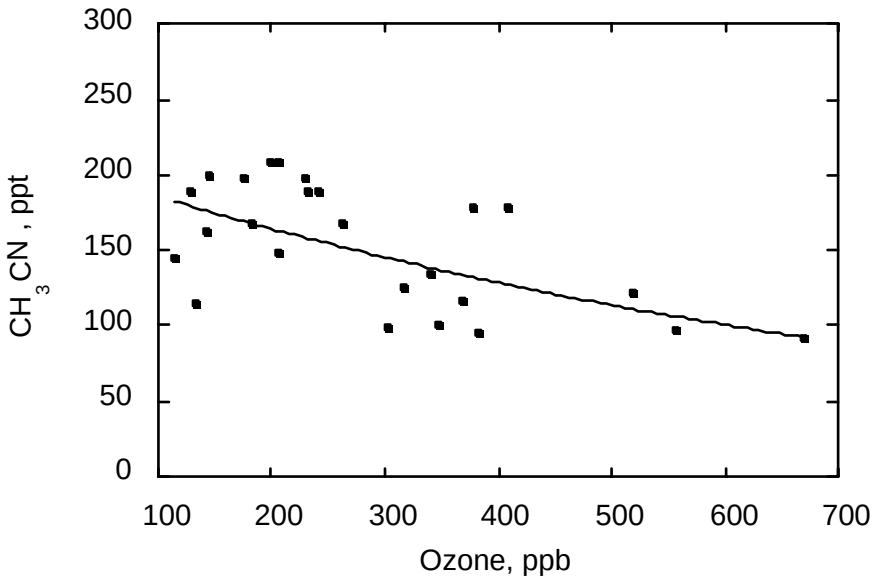

Figure 4: Methyl cyanide in the lowermost stratosphere

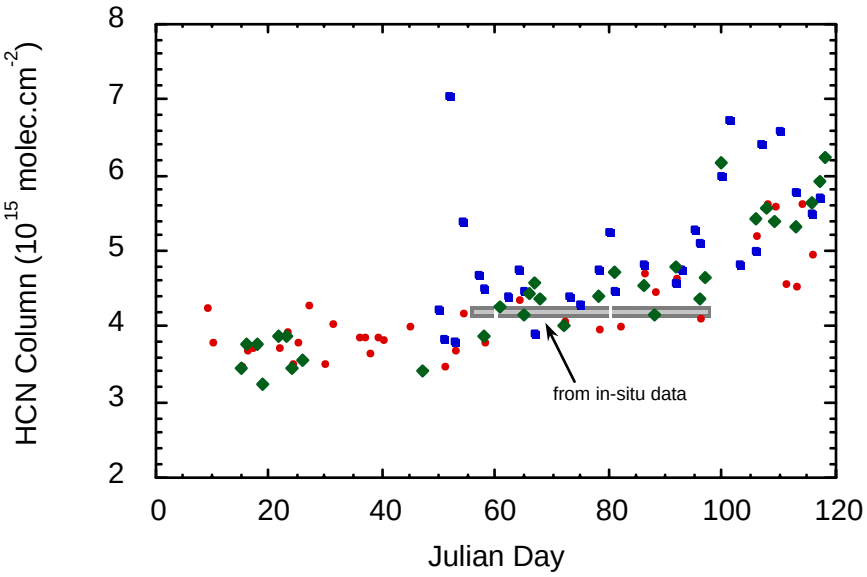

Figure 5: A comparison of the HCN columns (0-12 km) derived from spectroscopic observations over Japan with in-situ measurements over the Pacific. Shaded area represents the mean value derived from in-situ data. Red-Moshiri, Blue-Rikubetsu, Green- Tsukuba

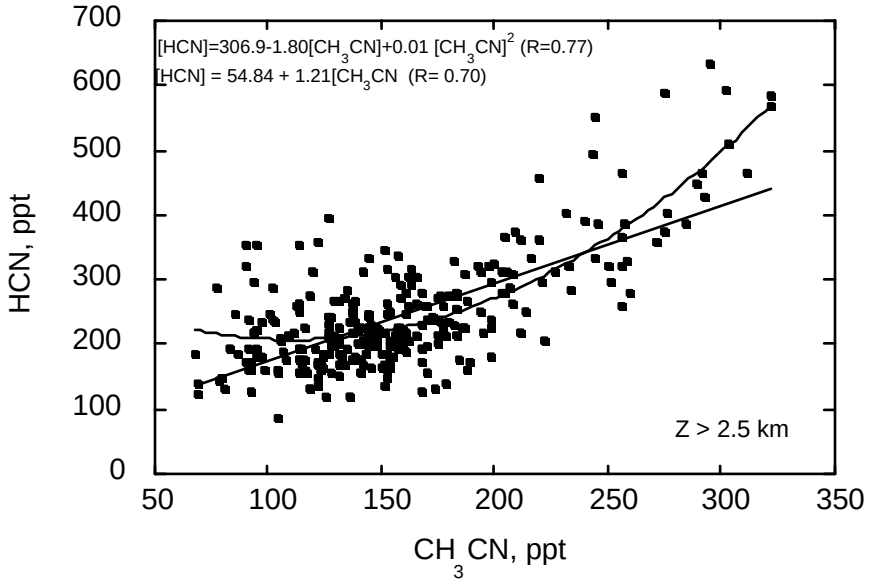

Figure 6: Relationship between the atmospheric mixing ratios of HCN and CH_3CN in the free troposphere

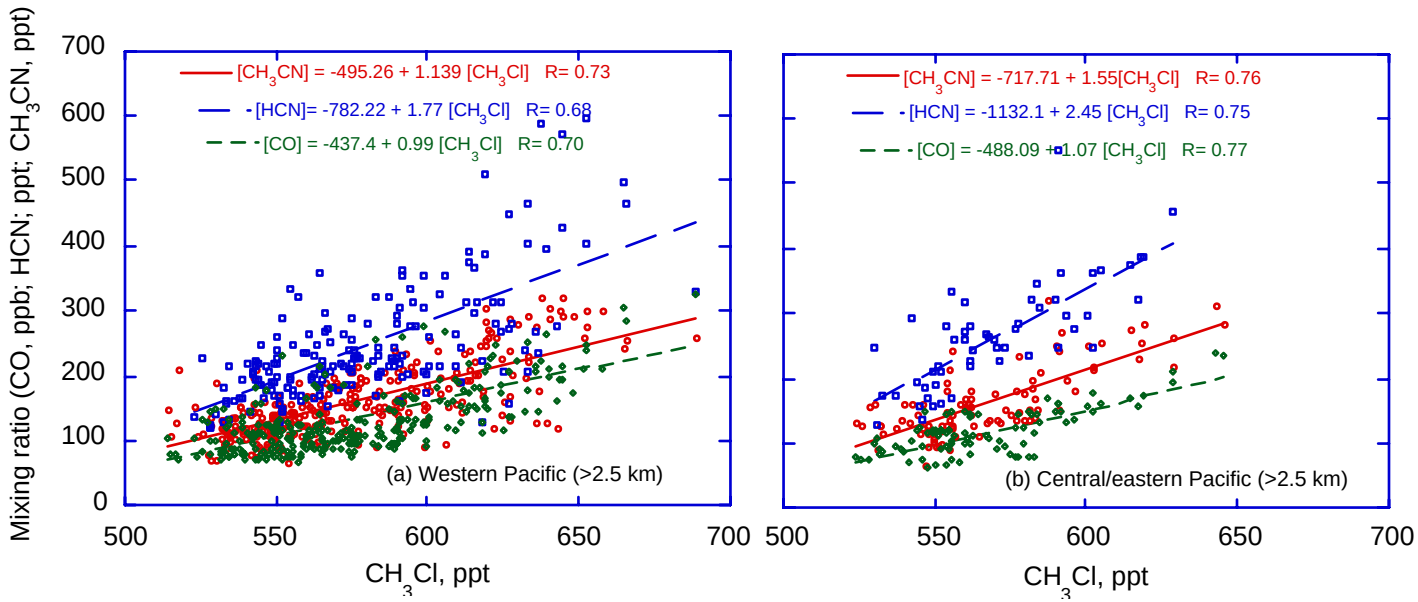

Figure 7: Relationships between the mixing ratios of methyl chloride with CH_3CN, HCN, and CO in the free troposphere over the western Pacific (a) and eastern/central Pacific (b). For the entire ensemble of data best fit slopes are $\Delta HCN/\Delta CH_3Cl$ -1.80; $\Delta CH_3CN/\Delta CH_3Cl$ -1.19; and $\Delta CO/\Delta CH_3Cl$ -1.00.

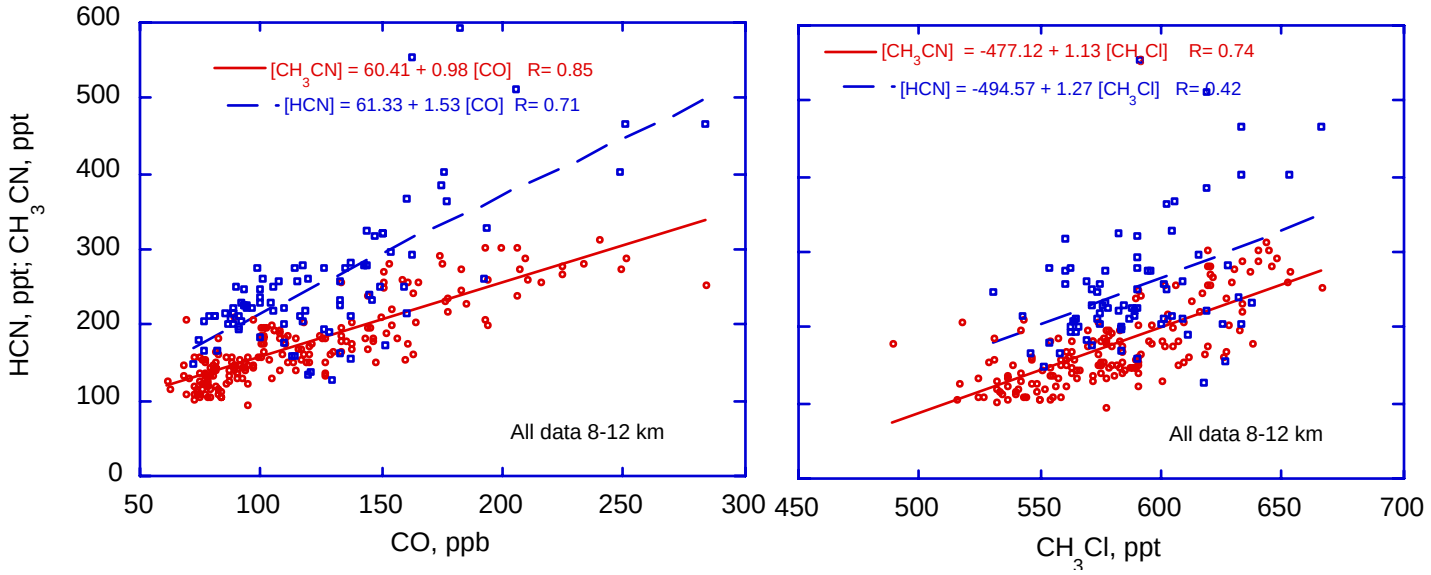

Figure 8: Relationship of HCN and CH_3CN with select tracers in the upper troposphere (8-12 km)

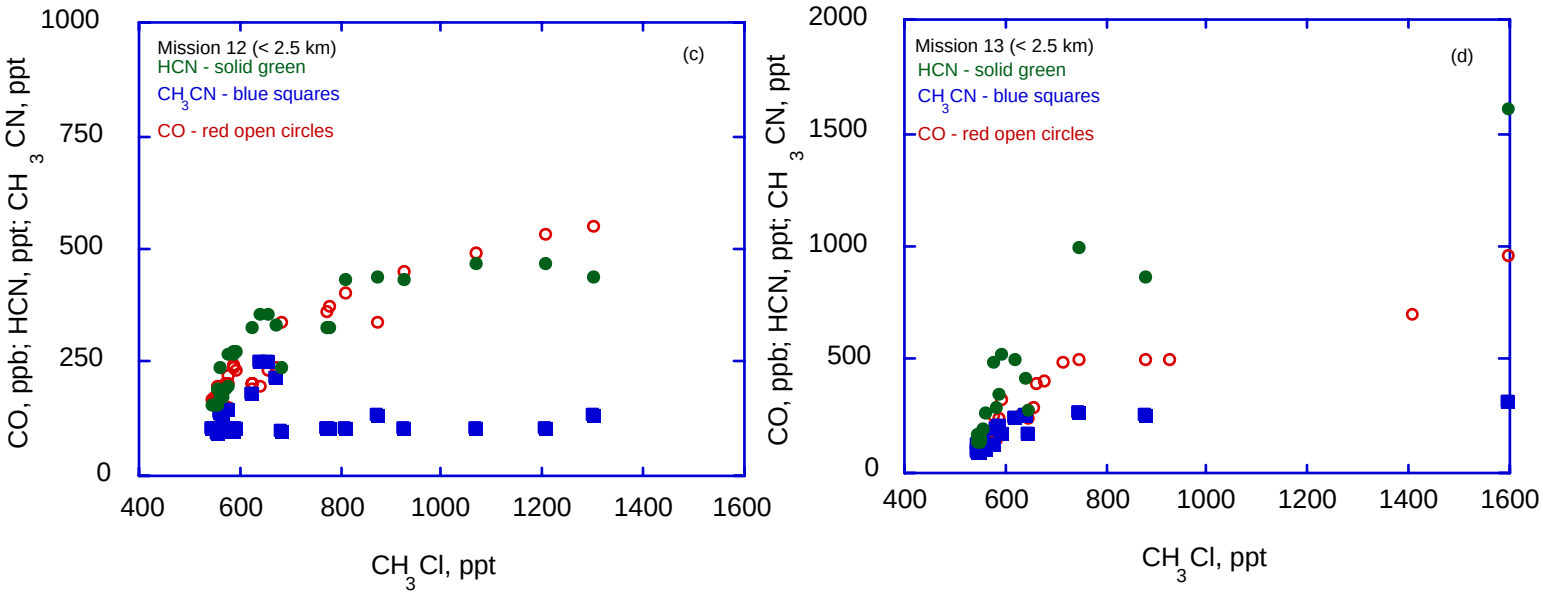

Figure 9: Relationships between the mixing ratios HCN and CH_3CN with select tracers in the boundary layer during two major pollution outflow episodes from China